



University of Utah

UNDERGRADUATE RESEARCH JOURNAL

INVESTIGATING MELT-ROCK INTERACTIONS IN GABBROIC ROCKS FROM THE ATLANTIS MASSIF: IMPLICATIONS FOR OCEANIC CRUSTAL ACCRETION

William Haddick, Sarah Lambart
Department of Geology and Geophysics

Background

Igneous petrologists have been using mid-ocean ridge basalts (MORB) and plutonic rocks at spreading ocean ridges as a tool to gain a better understanding of the upper mantle and crustal processes for the past forty years. Early assumptions to explain melt evolution in oceanic crustal magma chambers relied mostly on fractional crystallization. However, fractional crystallization cannot account for these processes alone as MORB is likely to undergo many other modifications prior to eruption, such as magma-mixing or melt-rock reaction. This is evident in the complex nature of MORB's where major, minor and trace element chemical disequilibrium prevent petrologists from establishing fractional crystallization as the primary melt migration mechanism. Minor element investigations on gabbroic rocks located at the Hess Deep rift valley⁽¹⁾ support this assumption, where Cr_2O_3 contents in clinopyroxenes reach 1.11% within primitive MORB at the Hess Deep, inconsistent with $\sim 0.5\%$ Cr_2O_3 predicted for melts produced by fractional crystallization⁽¹⁾. Hence, melt-rock interactions should exert a significant role during oceanic crustal accretion and it has been suggested that reactive porous flow (RPF) could provide a better explanation for melt evolution at fast-spreading ridges⁽²⁾. RPF suggests that migrating oceanic melts react as they travel upwards through a crystalline mush containing a small percentage of melt (Fig. 1).

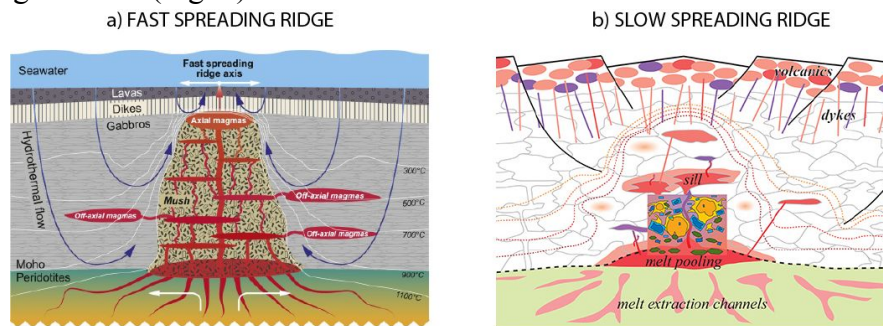


Figure 1. Conceptual models for melt circulation at (a) a fast spreading ridge⁽¹⁾ and (b) a slow-spreading ridge⁽⁵⁾. In fast spreading ridges, a large mush zone exists where intensive magma-rock reaction could occur. At slow spreading ridges, the mush zone could be significantly smaller and individual pools of melt could crystallize forming small gabbroic intrusions and potentially limiting melt rock reactions.

The Atlantis Massif provides a unique opportunity to determine if RPF can occur during crustal accretion at a slow-spreading ridge. The massif is a large undersea dome formed 1.5 to 2 million years ago from low angle detachment faulting along a transform boundary, located at the

Mid-Atlantic Ridge⁽³⁾. The eastern portion of the massif contains volcanics within the hanging wall, while the central and southern portions contain intrusives characteristic of an ultramafic oceanic core complex in the footwall⁽³⁾. In 2004 and 2005, the Integrated Ocean Drilling Program (IODP) carried out expeditions 304 and 305 to extract core samples from the Atlantis Massif within the footwall⁽³⁾. The main hole, Hole U1309D, penetrated 1415.5 mbsf (meters below sea floor) and recovery averaged 75%⁽³⁾. Over 96% of Hole U1309D is made up of gabbroic rock types (Fig. 2), which consist of the most primitive and freshest plutonic rocks recovered from the ocean floor⁽⁵⁾. In an attempt to characterize the intra-sample chemical disequilibrium, major element profiles were constructed on adjacent clinopyroxene and plagioclase grains within these gabbroic rocks using electron microprobe analysis (EMPA). These results will then be combined with data recovered from trace element analysis via Laser Ablation-Inductively Coupled Plasma-Mass Spectrometry (LA-ICP-MS), and utilized in a Magnesium-Rare Earth Element (Mg-REE) geospeedometer⁽⁴⁾ to construct a thermal history for the Atlantis Massif.

Method

Petrographic analysis

Out of the thirty total samples, nine were selected for EMPA and LA-ICP-MS analysis from petrographic observations summarized in Table 1. Selection criteria were: medium to large grain size (>5mm), low degree of alteration, and evidence for intra sample or intra crystal chemical zoning. An Olympus BHA cross polarized microscope was used to locate adjacent grains of clinopyroxene and plagioclase.

Table 1. *Petrographic observations made with an Olympus BHA cross polarized microscope*

Sample	Grain Size	Degree of Alteration	Chemical zoning
73R2 124-129	Large	Moderate	N/A*
90R3 22-26	Large	Moderate	Mg-Ti core to rim zoning in cpx
174R1 86-89	Large	Low	Fe zoning east to west in cpx
214R1 128-133	Small	Moderate	N/A
250R1 83-87	Large	Low	N/A
250R2 60-66	Large	Moderate-High	N/A
262R2 35-39	Large	Moderate	Cr-Ti core to rim zoning in olv
268R3 6-12 (large)	Large	Low	N/A
268R3 6-12 (small)	Medium	High	N/A

*N/A is noted for samples who either had faulty elemental maps or did not have elemental maps
Microprobe analyses

Major element analyses took place where linear profiles were set across adjacent grains of clinopyroxene and plagioclase in the nine samples selected during petrographic analysis to determine major element weight percents using EMPA. Samples were carbon coated (~20 nm thick). Profiles across adjacent clinopyroxene and plagioclase grains were characterized using a Cameca SX100 electron microprobe (Fig 2).

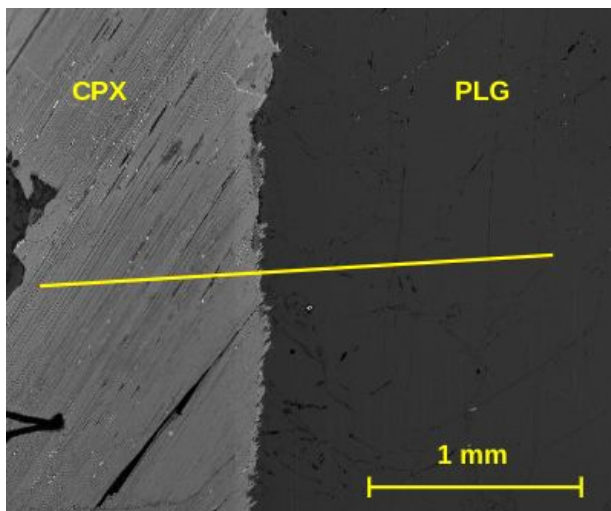


Figure 2. Backscatter electron (BSE) image of a major element profile ran across clinopyroxene (CPX) and plagioclase (PLG) grains in sample 73R2 124-129 using a Cameca SX100 electron microprobe.

In situ analyses were performed using a 15 keV accelerating voltage, and 10 μm diameter spot size with the following mineral and oxide standards: diopside (Ca, Mg, Si), sanidine (Al, K), San Carlos olivine (Mg, Fe), rhodonite (Mn), rutile (Ti), chromite (Cr), apatite (P), and celestite (S). Counting times were 10s on peak for Na, 25s on peak for Si, Al, Mn, Fe, K, Ca, and Mg, and 40s on peak for Ti, Cr, P, and S. Half of the peak time were used on high and low backgrounds. Each profile was approximately 1500-2000 μm in length (one profile was set at 7800 μm) with a ~100 μm step. San Carlos olivine was analyzed as a secondary standard before and after each profile to help remove inter-session variability.

Results

Despite multiple calibrations, the oxide totals in major element analyses were high (on average 101.95% +/- 3.17% for clinopyroxene, and 101.48% +/- 3.35% for plagioclase). Consequently, analyses with totals lower than 98% and higher than 105% were rejected. Analyses showing obvious signs of contamination (e.g. MgO > 1 wt % in plagioclase) were also rejected. Data reported in Table 2 are analyses collected for each profile that passed through these filters.

Table 2. Average totals for anorthite content in plagioclase (column 3) Mg # in clinopyroxene (column 4) and Cr₂O₃/TiO₂ ratio in clinopyroxene (column 5) for profiles that underwent major element analysis via a Cameca SX100 electron microprobe

Sample ID	Profile ID	An (%)	Mg #	Cr ₂ O ₃ /TiO ₂
73R2 124-129	P2C-1	71.99	80.15	0.77
	C2P-2	81.68	81.36	0.88
90R3 22-26	P2C-1	76.19	82.73	1.00
	P2C-2	69.96	83.98	0.47
	C2P-3	74.57	82.10	0.86
174R1 86-89	P2C-1	60.56	77.37	0.64
	P2C-2	60.41	80.07	0.76
214R1 128-133	P2C2P-1	70.71	84.67	0.57
	P2C-2	69.43	86.04	0.50
250R1 83-87	C2P-1	74.86	80.09	0.56
	P2C-2	73.25	84.06	2.16
242R2 35-39	C2P-1	72.55	82.39	2.09
	P2C-2	72.84	80.49	2.63
268R3 6-12 (large)	C2P-1	64.30	77.39	0.22
	P2C2P-2	70.62	80.97	2.07
268R3 6-12 (small)	P2C2P-1	67.31	74.97	0.15
	P2C-2	60.51	80.95	0.12
	P2C2P-3	69.99	84.94	0.44
	P2C2P-4	67.79	84.31	0.49
	C2P-5	72.09	86.42	1.85

Figure 3a presents the log of the U1309D with the locations of the nine selected samples indicated with colored circles. For each sample, Figure 3b-d present the range of Anorthite (An) content in plagioclase and Mg# and Cr₂O₃/TiO₂ ratio in clinopyroxene for each profile.

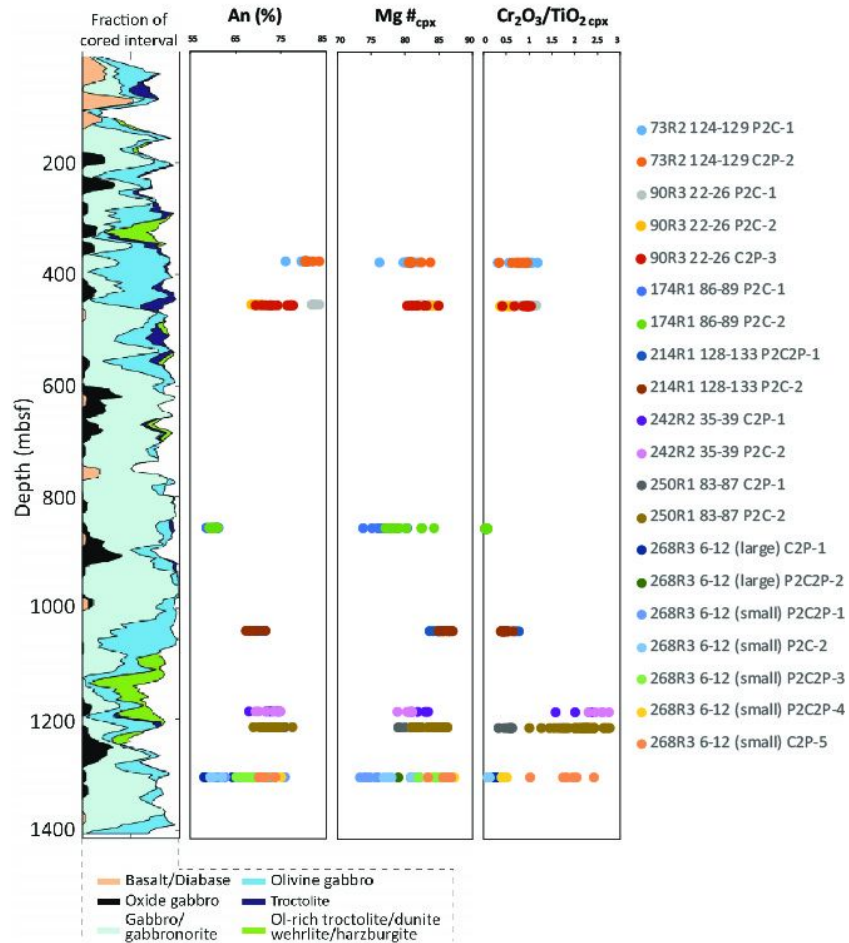


Figure 3. Depth log for samples recovered at hole U1309D showing (a) lithologies, (b) anorthite % in plagioclase, (c) Mg # in clinopyroxene, (d) Cr₂O₃/TiO₂ ratio in clinopyroxene.

In Figure 4, four profiles were selected which plot the chemical variation (An in plagioclase, Mg# and Cr₂O₃/TiO₂ ratio in clinopyroxene) from core to core.



Figure 4. Major element profiles showing anorthite percentage in plagioclase (An %), Mg# in clinopyroxene, and Cr₂O₃/TiO₂ ratio in clinopyroxene.

Discussion

High oxide totals present during major element analysis introduce some degree of error in representing anorthite percentage, Mg #, and $\text{Cr}_2\text{O}_3/\text{TiO}_2$ totals within these samples. However, even with this marginal degree of error, chemical disequilibrium is still observed between adjacent plagioclase and clinopyroxene grains within samples recovered at the Atlantis Massif. This chemical disequilibrium is observed at the core log, profile, and mineral grain scales.

At the core log scale, there appears to be no systematic trends with depth for anorthite percentage, Mg #, and $\text{Cr}_2\text{O}_3/\text{TiO}_2$ totals across all nine samples that were analyzed, as depicted in Figure 3. This indicates that fractional crystallization is not present as the main melt migration mechanism for this massif, since fractional crystallization predicts a linear trend of primitive (larger) values near the surface with more differentiated (lower) values as depth increases.

Figure 4 depicts chemical variability at the profile scale across adjacent plagioclase and clinopyroxene grains. An example of this is the systematic increase in anorthite percentage in plagioclase in comparison to the flat consistent Mg # observed in clinopyroxene for profile 73R2 124-129. Another example is seen between the two profiles in sample 268R3 6-12 (large), where $\text{Cr}_2\text{O}_3/\text{TiO}_2$ ratios in profile C2P-1 average out at 0.22 while reaching up to an average of 2.07 in profile P2C2P-2. This is an interesting result considering these two profiles in sample 268R3 6-12 (large) are separated by approximately 3 centimeters.

Examples of chemical disequilibrium at the mineral scale are also observed in Figure 4, where Mg # and $\text{Cr}_2\text{O}_3/\text{TiO}_2$ decoupling in clinopyroxene occurs in all four profiles. Along with this, a high degree of anorthite percentage in plagioclase is observed for profile 268R3 6-12 (large), in comparison to the lower and consistent anorthite percentages in profile 174 86-89 P2C-1.

Conclusions

MORB's and plutonic rocks recovered at spreading ocean ridges provide a unique challenge in understanding melt migration mechanisms for these magma chambers. Chemical disequilibrium prevalent within mineral grains at these locations prevent petrologists from describing thermal histories exclusively through fractional crystallization. Major element analysis that took place between adjacent plagioclase and clinopyroxene grains within gabbroic rocks recovered at the Atlantis Massif quantifies and confirms this chemical disequilibrium taking place at the core log, profile, and mineral grain scales. Plausible explanations for this chemical variability include melt-rock interactions, magma mixing, and multiple melt injection sites during development of these magma chambers. The next step in compiling a thermal history for the Atlantis Massif is acquisition of trace element data, through LA-ICP-MS analysis. This trace element data will then be combined with major element data acquired through EMPA and utilized in a Mg-REE coupled geospeedometer to estimate crystallization temperatures, which will then be compared to previous studies conducted on the East Pacific Rise, a fast spreading ocean ridge.

References

- (1) Lissenberg, C Johan, et al. "Pervasive Reactive Melt Migration through Fast-Spreading Lower Oceanic Crust (Hess Deep, Equatorial Pacific Ocean)." *Earth and Planetary Science Letters* 361, 2012, pp. 436–477.
- (2) Lissenberg, C Johan, and Christopher J MacLeod. "A Reactive Porous Flow Control on Mid-Ocean Ridge Magmatic Evolution." *Journal of Petrology*, vol. 57, no. 11 & 12, 2016, pp. 2195–2220.
- (3) Miller, Dee J, et al. "Oceanic Core Complex Formation, Atlantis Massif, Mid-Atlantic Ridge: Drilling into the Footwall and Hanging Wall of a Tectonic Exposure of Deep, Young Oceanic Lithosphere to Study Deformation, Alteration, and Melt Generation." *Proceedings of the Integrated Ocean Drilling Program*, 304/305, 2004.
- (4) Sun, C., and C. J. Lissenberg, "Formation of Fast-Spreading Lower Oceanic Crust as Revealed by a New Mg–REE Coupled Geospeedometer." *Earth and Planetary Science Letters* 487, 2018, 165–178 (2017)
- (5) Blackman, D. K. et al. Drilling constraints on lithospheric accretion and evolution at Atlantis Massif, Mid-Atlantic Ridge 30°N. *J. Geophys. Res.* 116, B07103 (2011).